

Measurements of the branching fractions and charge asymmetries of charmless three-body charged B decays

(Dated: February 7, 2003)

We present measurements of branching fractions and charge asymmetries for charged B meson decays to three-body final states of charged pions and kaons, using 81.8 fb^{-1} of data collected at the $\Upsilon(4S)$ resonance with the *BABAR* detector at the SLAC PEP-II asymmetric B Factory. No assumptions are made about intermediate resonances. We measure the branching fractions $\mathcal{B}(B^+ \rightarrow \pi^+\pi^-\pi^+) = (10.9 \pm 3.3 \pm 1.6) \times 10^{-6}$, $\mathcal{B}(B^+ \rightarrow K^+\pi^-\pi^+) = (59.1 \pm 3.8 \pm 3.2) \times 10^{-6}$, and $\mathcal{B}(B^+ \rightarrow K^+K^-\pi^+) = (29.6 \pm 2.1 \pm 1.6) \times 10^{-6}$, where the first uncertainty is statistical and the second uncertainty is systematic. We also measure the charge asymmetries $\mathcal{A}(B^+ \rightarrow \pi^+\pi^-\pi^+) = -0.39 \pm 0.33 \pm 0.12$, $\mathcal{A}(B^+ \rightarrow K^+\pi^-\pi^+) = 0.01 \pm 0.07 \pm 0.03$ and $\mathcal{A}(B^+ \rightarrow K^+K^-\pi^+) = 0.02 \pm 0.07 \pm 0.03$. In the same study, we do not observe a significant signals for the final state $B^+ \rightarrow K^+K^-\pi^+$ and the Standard Model suppressed modes $B^+ \rightarrow K^-\pi^+\pi^+$ and $B^+ \rightarrow K^+K^+\pi^-$, and therefore provide the 90% confidence upper limits $\mathcal{B}(B^+ \rightarrow K^+K^-\pi^+) < 6.3 \times 10^{-6}$, $\mathcal{B}(B^+ \rightarrow K^-\pi^+\pi^+) < 1.8 \times 10^{-6}$ and $\mathcal{B}(B^+ \rightarrow K^+K^+\pi^-) < 1.3 \times 10^{-6}$.

The study of charmless hadronic B decays can make important contributions to the understanding of CP violation in the Standard Model, as well as to models of hadronic decays. There has been recent theoretical progress on using three-body decays to measure direct CP violation and to extract the Cabibbo-Kobayashi-Maskawa (CKM) angle γ [1]. Measurements of the decay $B^+ \rightarrow \pi^+\pi^-\pi^+$ can also be used to reduce the uncertainties in the measurement of the CKM angle α [2]. We present results on the branching fractions and charge asymmetries of charged B meson decays to three-body final states of charged pions and kaons [3], with no assumptions about intermediate resonances and with open charm contributions subtracted. Upper limits and measurements of some of these branching fractions have been performed previously with somewhat fewer statistics [4].

The data used in this analysis were collected at the PEP-II asymmetric e^+e^- storage ring with the *BABAR* detector, described in detail elsewhere [5]. Charged particles are detected, and their momenta measured, with a 40-layer drift chamber (DCH) and a five-layer silicon vertex tracker (SVT), both operating in a 1.5 T solenoidal magnetic field. Surrounding the DCH is a detector of internally reflected Cherenkov radiation (DIRC), and outside this is a CsI(Tl) electromagnetic calorimeter (EMC). The iron flux return of the solenoid is instrumented with resistive plate chambers. The data sample consists of 88.8 million $B\bar{B}$ pairs, corresponding to an integrated luminosity of 81.8 fb^{-1} collected at the $\Upsilon(4S)$ resonance (on-resonance) during the 2000-2002 run. In addition, a total integrated luminosity of 9.6 fb^{-1} was taken at 40 MeV below the $\Upsilon(4S)$ resonance (off-resonance), and was used to characterise the backgrounds from e^+e^- an-

nihilation into light $q\bar{q}$ pairs. We assume that the $\Upsilon(4S)$ decays equally to neutral and charged B meson pairs.

Hadronic events are selected based on track multiplicity and event topology. Backgrounds from non-hadronic events are reduced by requiring the ratio of Fox-Wolfram moments H_2/H_0 [6] to be less than 0.98. Candidate B decays are formed by combining three charged tracks, where each track is required to have at least 12 hits in the DCH, a maximum momentum of 10 GeV/ c , a minimum transverse momentum of 100 MeV/ c , and to originate from the beam-spot.

Signal decays are identified using two kinematic variables, the difference ΔE between the centre-of-mass (CM) energy of the B candidate and $\sqrt{s}/2$, where \sqrt{s} is the total CM energy, and the beam-energy substituted mass $m_{\text{ES}} = \sqrt{((s/2 + \mathbf{p}_i \cdot \mathbf{p}_B)^2/E_i^2 - \mathbf{p}_B^2)}$, where the B momentum \mathbf{p}_B and the four-momentum of the initial state (E_i, \mathbf{p}_i) are defined in the laboratory frame. For this analysis, we assume the appropriate mass hypothesis for each charged track in a given decay mode under study in calculating ΔE . For signal events, ΔE and m_{ES} are Gaussian distributed with resolutions of 20 MeV and 2.7 MeV/ c^2 , respectively. The typical ΔE separation between modes that differ by substituting a kaon for a pion in the final state is 45 MeV.

Charged pions and kaons are identified using dE/dx information from the SVT and DCH, and, for tracks with momenta above 700 MeV/ c , the Cherenkov angle and number of photons measured by the DIRC. Kaons are selected with requirements made on the product of the likelihood ratios determined from these measurements. The efficiency of selecting kaons is approximately 80%, which includes the geometrical acceptance, while the probabil-

ity of mis-identifying pions as kaons is below 5%, up to a momentum of 4.0 GeV/ c . This means that the probability of a kaon being mis-identified as a pion is 20%. Pions are required to fail both the kaon selection and an electron selection algorithm based on information from dE/dx , shower shapes in the EMC and the ratio of the shower energy and track momentum. The probability of mis-identifying electrons as pions is approximately 5%.

Since we are interested only in charmless decays, we veto candidates that contain charm mesons. This is done by removing B candidates when the invariant mass of the combination of any two of its daughter tracks (of opposite charge) is within 6σ of the mass of the D^0 meson and within 3σ of the mass of the J/ψ , $\psi(2S)$ or χ_{c0} mesons [7]. Here, σ is 10 MeV/ c^2 for D^0 , 15 MeV/ c^2 for J/ψ and $\psi(2S)$, and 18.3 MeV/ c^2 for χ_{c0} . All possible kaon and pion combinations are tested for the D^0 veto, while only the K^+K^- and $\pi^+\pi^-$ hypotheses are tested for the J/ψ , $\psi(2S)$ and χ_{c0} vetoes. The feed-through from J/ψ and $\psi(2S)$, which is less than one event for each signal channel, are from leptonic decays, in which the leptons have been mis-identified as pions or kaons.

In addition to these candidate selection requirements, we need to suppress backgrounds from light quark and charm continuum production. We reduce these by imposing requirements on two topological event shape variables computed in the $\Upsilon(4S)$ rest frame.

The first event shape variable is the cosine of the angle θ_T^* between the thrust axis of the selected B candidate and the thrust axis of the rest of the event, i.e. all charged tracks and neutral particles not originating from the B candidate. For continuum backgrounds, the directions of the two axes tend to be aligned because the daughters of the reconstructed candidate generally lie along the dijet axis of such events. Therefore, the distribution of $|\cos\theta_T^*|$ is strongly peaked towards unity. The low CM momentum of the B mesons in the $\Upsilon(4S)$ decay means that the distribution of $|\cos\theta_T^*|$ is uniform for signal events. The difference in the $|\cos\theta_T^*|$ dependence allows us to discriminate between signal B decays and continuum background.

The second event shape variable is a Fisher discriminant [8], which is formed from the summed scalar momenta of all charged and neutral particles from the rest of the event within nine nested cones coaxial with the thrust axis of the B candidate. The parameters for the Fisher discriminant are chosen to maximise the separation between signal and background events, and are calculated for each signal mode separately using Monte Carlo simulated signal and light quark continuum events.

The selection criteria for the event shape variables are optimised separately for each signal mode to achieve maximum sensitivity for the branching fraction.

Despite the above event shape variables rejecting over 90% of the $q\bar{q}$ background, there is still a significant number of these events that must be subtracted to extract a

signal. The residual background level is estimated from the observed number of events in a sideband region, located near to the signal region in the $m_{ES} - \Delta E$ plane, and extrapolating into the signal region. The shape of the m_{ES} distribution of the background is parameterised according to the phenomenologically motivated ARGUS function [9], and is measured using off-resonance data and the upper sideband in the ΔE variable in on-resonance data ($0.10 < \Delta E < 0.25$ GeV). A quadratic function is used to parameterise the ΔE distribution of the background. The product of the ratios of the areas under the shape functions in ΔE and m_{ES} in the signal and sideband regions, R , gives the ratio of the number of background events in the two areas.

The branching fraction for each channel is measured over the whole Dalitz plot, which is divided into cells of equal area (1 GeV^2) to enable us to find the selection efficiency as a function of position in the Dalitz plot. Taking ϵ_i to be the efficiency of reconstructing the signal in the i^{th} bin in the Dalitz plot, determined from Monte Carlo simulated events, the branching fraction for each signal mode is given by:

$$\mathcal{B} = \frac{1}{N_{B\bar{B}}} \left(\sum_i \frac{(N_{1i} - RN_{2i} - N_x \epsilon_i'')}{\epsilon_i} - n_x - n_b \right), \quad (1)$$

where N_{1i} and N_{2i} are the number of events observed in the signal and grand sideband (GSB) regions, respectively, while N_x , ϵ_i'' , n_x and n_b are background contributions that are defined below. No significant differences were found for the value of R in different regions of the Dalitz plot, so an average value is used for all bins.

The probability of a kaon being mis-identified as a pion is 20%, which includes the efficiency of the particle identification algorithm and the geometrical acceptance. This means there is significant cross-feed into the signal region from the decay mode that has one more kaon, which is subtracted for each bin, i . This is represented by the $N_x \epsilon_i'' / \epsilon_i$ term in Eq. 1, where N_x is the total number of events that is the source of the cross-feed, and ϵ_i'' is the probability for the cross-feed events to pass the selection criteria. The latter is determined from Monte Carlo simulation by generating decays across the Dalitz plot weighted by the number of events observed in on-resonance data and determining the cross-feed selection efficiency in each bin.

In addition to the cross-feed where only one of the kaon tracks is misidentified as a pion, there can also be cross-feed where either two kaons are mis-identified as pions (probability of 4%), or one of the pions is mis-identified as a kaon (probability of 2%). These are smaller, second-order effects, and so it is adequate to subtract the average number of efficiency-corrected events over the whole Dalitz plot. This is represented by the n_x term in Eq. 1.

Finally, the n_b term represents the small number of other $B\bar{B}$ backgrounds that are subtracted: from D^0

TABLE I: Branching fraction results for on-resonance data. The various quantities and their uncertainties are explained in the text.

Signal Mode	$\pi^\pm\pi^+\pi^\pm$	$K^\pm\pi^+\pi^\pm$	$K^\pm K^+\pi^\pm$	$K^\pm K^+K^\pm$	$K^+\pi^\pm\pi^\pm$	$K^\pm K^\pm\pi^+$
$\sum_i N_{1i}$	1029	1502	733	646	494	209
$\sum_i N_{2i}$	5577	5209	4012	1308	3268	1025
$\langle\epsilon\rangle(\%)$	12.7 ± 0.5	12.8 ± 1.4	13.9 ± 0.9	14.9 ± 0.9	18.5 ± 0.9	15.3 ± 0.7
R	0.144 ± 0.003	0.146 ± 0.003	0.150 ± 0.003	0.158 ± 0.006	0.155 ± 0.003	0.157 ± 0.006
1) $\sum_i N_{1i}/\epsilon_i$	7597 ± 275	11056 ± 327	5071 ± 216	4011 ± 182	2670 ± 120	1366 ± 94
2) $\sum_i RN_{2i}/\epsilon_i$	$5938 \pm 94 \pm 117$	$5604 \pm 89 \pm 111$	$4041 \pm 72 \pm 80$	$1381 \pm 46 \pm 55$	$2738 \pm 48 \pm 53$	$1052 \pm 33 \pm 40$
3) $\sum_i N_x \epsilon_i''/\epsilon_i$	$474 \pm 33 \pm 40$	$22 \pm 1 \pm 30$	$671 \pm 15 \pm 59$	—	—	344 ± 31
4) n_x	—	-189 ± 34	110 ± 128	—	—	53 ± 5
5) D^0 Bkgnd	216 ± 24	268 ± 28	47 ± 6	—	33 ± 5	31 ± 5
6) $\eta'K$ Bkgnd	—	106 ± 30	—	—	—	—
7) Signal Yield	$970 \pm 291 \pm 130$ $\pm 22 \pm 50$	$5246 \pm 339 \pm 127$ $\pm 39 \pm 247$	$202 \pm 227 \pm 163$ $\pm 16 \pm 9$	$2630 \pm 188 \pm 55$ $\pm 12 \pm 124$	$-101 \pm 129 \pm 53$ $\pm 0 \pm 5$	$-114 \pm 100 \pm 51$ $\pm 0 \pm 5$
$\mathcal{B} (\times 10^{-6})$	$10.9 \pm 3.3 \pm 1.6$	$59.1 \pm 3.8 \pm 3.2$	$2.3 \pm 2.6 \pm 1.8 (< 6)$	$29.6 \pm 2.1 \pm 1.6$	$-1.1 \pm 1.5 \pm 0.6$	$-1.3 \pm 1.1 \pm 0.6$
Significance (σ)	5.7	> 6	1.1	> 6	—	—
90% C.L.	—	—	< 6.3	—	< 1.8	< 1.3

candidates that lie outside the 6σ invariant mass window for $B^+ \rightarrow \pi^+\pi^-\pi^+$ and $B^+ \rightarrow K^+\pi^-\pi^+$, and $B^\pm \rightarrow \eta'(\rightarrow \rho^0\gamma)K^\pm$ events for the $B^+ \rightarrow K^+\pi^-\pi^+$ channel. We do not divide up the Dalitz plot into cells for the standard model suppressed modes $B^+ \rightarrow K^-\pi^+\pi^+$ and $B^+ \rightarrow K^+K^+\pi^-$, and instead use average values for the signal efficiency and cross-feed terms.

The signal region is defined to be $|m_{\text{ES}} - m_B| < 8 \text{ MeV}/c^2$ and $|\Delta E - \langle \Delta E \rangle| < 60 \text{ MeV}$, where $\langle \Delta E \rangle$ is the mean value of ΔE measured from on-resonance data for the calibration sample $B^- \rightarrow D^0\pi^-$, $D^0 \rightarrow K^-\pi^+$, and m_B is the nominal mass of the charged B meson [7]. The GSB region is defined to be $5.21 < m_{\text{ES}} < 5.25 \text{ GeV}/c^2$ and $|\Delta E - \langle \Delta E \rangle| < 100 \text{ MeV}$.

The branching fraction results are summarised in Table I, where the first four rows show the total number of events in the signal and GSB regions, the average signal efficiencies $\langle\epsilon\rangle$ and the values of R for each mode.

The row labelled 1 shows the sum over Dalitz plot bins of the number of events observed in the signal region divided by the signal efficiency, where the error is the statistical uncertainty of the number of signal events. The next row, labelled 2, shows the sum over Dalitz plot bins of the expected number of combinatorial background events divided by the signal efficiency. The errors shown for these values correspond to the statistical uncertainty in N_{2i} , and the systematic uncertainty for R , which arises from the limited statistics in the sideband region and off-resonance data.

Row 3 shows the expected background from cross-feed events, where a kaon has been mis-identified as a pion. The first and second errors on these quantities represent the systematic uncertainties in ϵ_i'' and N_x , respectively, except for channel $B^+ \rightarrow K^+K^+\pi^-$, where the uncertainty represents the average of the ϵ_i'' and

N_x contributions, since we did not divide up the Dalitz plot for this Standard Model suppressed mode. The $B^+ \rightarrow K^+K^-K^+$ and $B^+ \rightarrow K^-\pi^+\pi^+$ channels have negligible cross-feed backgrounds.

The second-order cross-feed terms n_x are shown in row 4, and the errors for these values are dominated by the uncertainties in the second-order cross-feed probabilities. Note that the n_x term for $B^+ \rightarrow K^+\pi^-\pi^+$ is negative, which compensates for the extra background events of $B^+ \rightarrow K^+K^-K^+$ decays that are mis-identified as $B^+ \rightarrow K^+K^-\pi^+$, which in turn pass the selection criteria for $B^+ \rightarrow K^+\pi^-\pi^+$.

Rows 5 and 6 show the expected backgrounds from D^0 and $\eta'K$ decays, where the error for each value includes the uncertainties in the selection efficiencies and the branching fractions for the background decays [7]. The sum of these two rows gives the value of n_b in Eq. 1.

Row 7 shows the signal yield, which is the subtraction of rows 2 to 6 from row 1. The first error is the combination of the statistical uncertainties for the number of events in the signal and GSB regions. The second error for the entries in row 7 corresponds to the quadrature sum of all the other systematic uncertainties from rows 2 to 6. The third error for row 7 is from the bin-by-bin uncertainty for the selection efficiency (not the average). This is zero for $B^+ \rightarrow K^-\pi^+\pi^+$ and $B^+ \rightarrow K^+K^+\pi^-$, since we only use the average efficiencies. The last error originates from the fractional systematic uncertainties for the signal efficiencies, which arise from charged-particle tracking ($\pm 0.8\%$ per track), event shape variable selections (± 1.0 to 2.5%), particle identification ($\pm 1.4\%$ and $\pm 1.0\%$ per pion and kaon track, respectively), and ΔE and m_{ES} ($\pm 1\%$).

The next row in Table I shows the branching fraction results, where the first errors are from the statistical un-

certainties on the number of events, while the second errors are the sum in quadrature of all systematic uncertainties. The significance of each branching fraction result is defined as the ratio of the signal yield to the total (statistical and systematic) uncertainty of the background in the signal region. We observe significant signals for the modes $B^+ \rightarrow \pi^+\pi^-\pi^+$, $B^+ \rightarrow K^+\pi^-\pi^+$ and $B^+ \rightarrow K^+K^-K^+$, and provide 90% C.L. upper limits for the other channels, using the formalism in [10]. As a consistency check, the branching fraction for the control sample $B^- \rightarrow D^0\pi^-$, $D^0 \rightarrow K^-\pi^+$ is measured to be $(190 \pm 3 \pm 10) \times 10^{-6}$, which agrees with the currently measured value of $(201 \pm 20) \times 10^{-6}$ [7].

Figure 1 shows the ΔE and m_{ES} projections for the signal region for each of the observed modes. Each plot shows the expected levels of continuum and $B\bar{B}$ background (solid and dashed lines, respectively).

We have also measured the charge asymmetries for the modes with observed signals using a method similar to that used for the branching fraction measurements. The charge asymmetries are defined as $\mathcal{A} = (N^- - N^+) / (N^- + N^+)$, where N^- (N^+) is the signal yield for negatively (positively) charged B candidates, as defined by Eq. 1. The normalisation factor $N_{B\bar{B}}$ cancels out in the asymmetry ratio, while the cross-feed and $B\bar{B}$ background contributions cancel in the asymmetry numerator, $(N^- - N^+)$. The measured charge asymmetries are $\mathcal{A}(B^+ \rightarrow \pi^+\pi^-\pi^+) = -0.39 \pm 0.33 \pm 0.12$, $\mathcal{A}(B^+ \rightarrow K^+\pi^-\pi^+) = 0.01 \pm 0.07 \pm 0.03$ and $\mathcal{A}(B^+ \rightarrow K^+K^-K^+) = 0.02 \pm 0.07 \pm 0.03$, where the first errors are statistical and the second errors are systematic, which include the charge bias of the tracking and particle identification selection requirements (1%). No significant charge bias was found for the combinatorial background and its extrapolation factor R , nor for the signal efficiency and its variation across the Dalitz plot. Nevertheless, a contribution due to the uncertainty from these sources was added in quadrature to the systematic uncertainties of the measured charge asymmetries.

In summary, the branching fraction for $B^+ \rightarrow \pi^+\pi^-\pi^+$ has been measured for the first time, and we also observe the channels $B^+ \rightarrow K^+\pi^-\pi^+$ and $B^+ \rightarrow K^+K^-K^+$. We observe no charge asymmetries in these decays.

We are grateful for the excellent luminosity and machine conditions provided by our PEP-II colleagues, and for the substantial dedicated effort from the computing organizations that support *BABAR*. The collaborating institutions wish to thank SLAC for its support and kind hospitality. This work is supported by DOE and NSF (USA), NSERC (Canada), IHEP (China), CEA and CNRS-IN2P3 (France), BMBF (Germany), INFN (Italy), NFR (Norway), MIST (Russia), and PPARC (United Kingdom). Individuals have received support from the A. P. Sloan Foundation, Research Corporation, and Alexander von Humboldt Foundation.

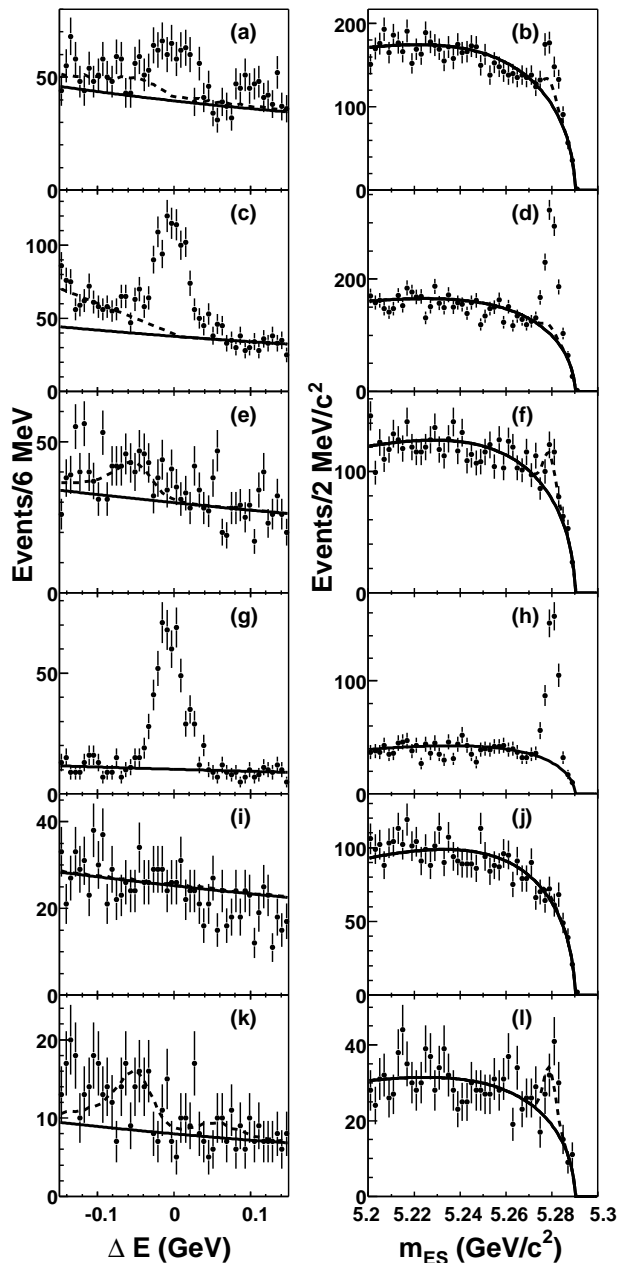


FIG. 1: Projections of ΔE and m_{ES} for $B^+ \rightarrow \pi^+\pi^-\pi^+$ (a and b), $B^+ \rightarrow K^+\pi^-\pi^+$ (c and d), $B^+ \rightarrow K^+K^-\pi^+$ (e and f), $B^+ \rightarrow K^+K^-K^+$ (g and h), $B^+ \rightarrow K^-\pi^+\pi^+$ (i and j) and $B^+ \rightarrow K^+K^+\pi^-$ (k and l) in the signal region. The solid curves show the $q\bar{q}$ background, while the dashed lines show the $B\bar{B}$ background.

- [1] R.E. Blanco, C. Gobel, and R. Mendez-Galain, Phys. Rev. Lett. **86**, 2720 (2001).
- [2] A.E. Snyder, H.R. Quinn, Phys. Rev. D **48**, 2139 (1993).
- [3] Throughout this paper, flavor-eigenstate decay modes imply also their charge conjugate.
- [4] CLEO Collaboration, T. Bergfeld *et al.*, Phys. Rev. Lett.

- 77**, 4503 (1996); BELLE Collaboration, K. Abe *et al.*, Phys. Rev. D **65**, 092005 (2002).
- [5] BABAR Collaboration, B. Aubert *et al.*, Nucl. Instr. and Meth. **A479**, 1 (2002).
- [6] G.C. Fox and S. Wolfram, Phys. Rev. Lett. **41**, 1581 (1978).
- [7] Particle Data Group, K. Hagiwara *et al.*, Phys. Rev. D **66**, 010001 (2002).
- [8] CLEO Collaboration, D. M. Asner *et al.*, Phys. Rev. D **53**, 1039 (1996).
- [9] The background for each mode is fit with $dN/dm_{\text{ES}} \propto m_{\text{ES}} \sqrt{1 - m_{\text{ES}}^2/E_{\text{beam}}^{*2}} \exp[-\xi(1 - m_{\text{ES}}^2/E_{\text{beam}}^{*2})]$, where E_{beam}^* is the on-resonance center-of-mass energy of the e^+ and e^- beams, equal to 5.29 GeV, and ξ is the shape parameter. This was introduced by the ARGUS Collaboration, H. Albrecht *et al.*, Z. Phys. C **48**, 543 (1990).
- [10] G.J. Feldman and R.D. Cousins, Phys. Rev. D **57**, 3873 (1998).